A. B. Sturm, P. Visintin and D. J. Oehlers

Design-oriented solutions for the shear capacity of reinforced concrete beams with and without fibers

Journal of Structural Engineering, 2021; 147(6):04021066-04021066

DESIGN ORIENTED SOLUTIONS FOR THE SHEAR CAPACITY OF REINFORCED CONCRETE BEAMS WITH AND WITHOUT FIBRES

[1]Sturm, A.B., [2]Visintin, P. and [3]Oehlers, D.J.

Published version found in ASCE Journal of Structural Engineering

DOI: https://doi.org/10.1061/(ASCE)ST.1943-541X.0003023

ABSTRACT

The inclusion of fibres substantially improves the shear resistance of reinforced concrete beams. Fibres can, therefore, be used as a partial or full substitute for traditional transverse reinforcement. Before replacement of traditional reinforcement with fibres can be undertaken, reliable expressions which incorporate the effect of fibres are required. In a previous study, a mechanics approach based on quantifying the pre-sliding shear capacity of fibre reinforced concrete beams was developed and broadly validated and compared to existing design approaches. While accurate, the numerical solution is too complicated for routine design and hence, in this paper, simplified solutions are developed. This is achieved by: (i) approximating the neutral axis depth at the initiation of shear failure, (ii) developing a closed-form solution for the angle of the critical diagonal shear crack, removing the need to iterate, and (iii) incorporating a simple approach to estimate the stress in the fibres crossing cracks, removing the need to integrate fibre stresses over a range of crack widths. To validate the simplified solutions, they are used to predict the capacity of tests on 626 reinforced concrete beams without stirrups, 176 reinforced concrete beams with stirrups and 23 fibre reinforced concrete beams. Importantly these simplified solutions largely retain the accuracy of the numerical approach and show an improved fit compared to currently available solutions.

INTRODUCTION

The design of reinforced concrete members is based on the assumption that ductile flexural failure always precedes brittle shear failure. As such, reliable approaches for predicting the shear capacity of a member and specifying the concrete and transverse reinforcement contributions to shear capacity are essential to the design process. With recent developments in concrete technology, the use of fibre reinforced concrete (FRC) has progressed significantly. Member level testing has identified a significant improvement in shear capacity can be achieved by the addition of fibres and it has been suggested that fibre reinforcement may reduce or entirely replace traditional transverse reinforcement (Casanova et al. 1997, Amin & Foster 2016).

To quantify the increase in shear capacity arising from fibre addition and, therefore, allow for the increased capacity to be considered in design practice, the Australian standard AS3600:2018 (Standards Australia 2018) includes expressions for quantifying the shear capacity of FRC members. In this approach: simplified modified compression field theory is applied to predict the concrete contribution to the shear capacity; a traditional truss model is used to determine the steel contribution; and a constant stress in the fibres is used to simulate the fibre contribution. Additional empirical factors are included to account for fibre orientation and size effect on the tensile stress in the fibres. The primary criticism here is that the model is based on simplified modified compression field theory. This approach assumes that aggregate interlock is the primary contributor to the shear capacity, and that the loss of aggregate interlock causes shear failure. In contrast to modified compression theory it has been suggested, including in the approach developed here, that the primary contributor to the shear capacity is the uncracked concrete above the crack tip (Volgyi & Windisch 2017; Donmez et al. 2020). The fib Model Code 2010 (fib 2012) also includes an expression to determine the shear capacity which considers the concrete and fibre contribution together based on the expression for shear capacity in the Eurocode 2 (CEN 2004). This expression is empirical in nature, hence difficult to extend to new materials. The fib Model Code 2010 (fib 2012) also outlines an alternative approach in the commentary based on simplified modified compression field theory similar to the approach in AS3600:2018 and therefore has similar issues. The Association Francaise de Genie Civil (AFGC 2013) has developed shear capacity expressions for ultra-high performance fibre reinforced concrete beams. In this approach, the shear capacity is increased by the vertical component of the force in the fibres; the stress in the fibres is taken as the average stress when the flexural strength is achieved and the force in the fibres is assumed to be perpendicular to the principal compressive stress. The concrete component of the shear capacity is also empirical hence difficult to extend to new materials. This is recognised as an additional capacity reduction factor is provided as the equation is extrapolated from that used for high strength concrete.

A mechanics based approach is desirable as it is difficult to extend empirical approaches outside the bounds from which they were calibrated (Lansoght 2019) hence a survey of mechanical approaches is also provided. These include Voo et al. (2006) which assumes a plastic distributions of stress in tension and compression along critical diagonal shear crack to determine the shear capacity. The primary issue with this approach is that it relies on the definition of effectiveness factors that would need to be calibrated for each new material.

The approach by Choi et al. (2007) calculates the concrete contribution to the shear capacity as a function of the shear force required to crack the flexural compression region and the fibre contribution as a function of a constant stress imposed on an inclined crack. This approach is based on a similar mechanism to Zhang et al. (2016a,b), where failure is controlled by the shear-compression failure of the flexural compression region. Unlike Zhang's approach, Choi et al. (2007) assumes a fixed 45° crack angle in the flexural tension region whereas in reality this can vary and the contribution of the fibres is determined based on single fibre pullout results. Single fibre pullout data is not always available and hence a model that uses the tensile properties obtained at the material scale is preferable because both AS3600:2018 (Standards Australia 2018) and the fib Model Code 2010 (fib 2012) consider either direct or indirect testing of the tensile material properties to be essential for characterising the material behaviour of FRC. A further limitation of the Choi's approach is that it requires iteration to determine the neutral axis depth and top fibre strains, but for a design approach it is desirable that iteration be avoided if possible.

Lee et al. (2016) suggested an approach in which the shear demand and capacity attributed to the compression zone and tension zone is determined and shear failure occurs when demands exceed the capacity in either region. This model attempts to combine the approaches which propose a shear failure mechanism of aggregate interlock in the flexural tension region and shear compression failure in the flexural compression region by attributing a proportion of the shear resistance to each mechanism. The primary issue in this approach is that it has been argued that the shear-compression failure is the dominant mechanism, for example see Volgyi & Windisch (2017) and Donmez et al. (2020) and hence aggregate interlock has minor influence on the shear capacity.

Zhang et al. (2016c) suggested an approach based on simplified modified compression field theory, in which the stress in the fibres is determined as a function of the bond strength of a single fibre obtained from single fibre pullout tests. The same criticisms exist here as for the previous modified compression field theory based approaches. In addition to these issues, the need for single fibre pullout tests rather than either direct or indirect tension tests results complicates the testing required to implement the model.

Foster & Barros (2018) also adapted simplified modified compression field theory where the contribution of the fibres is determined by considering the pullout of a single fibre where the inclination angle of the individual fibres with respect to the crack was considered. The same criticisms hold as for Zhang et al. (2016c). In addition this model requires data on the pullout of fibres at a range of angles to the crack face. This adds further complication to the testing to implement the model.

In response to criticisms of existing shear design approaches a new model to quantify the shear strength of FRC where the resistance of the flexural compression region is determined from the shear friction material properties was proposed by Sturm et al. (2020), with this approach being consistent with that developed by Zhang et al. (2016a,b) for ordinary reinforced concrete beams with steel or FRP reinforcement. When compared to existing methods (Voo et al. 2006; Choi et al. 2007; Lee et al. 2016; Zhang et al. 2016c; Foster & Barros 2018) for quantifying the shear strength of 29 FRC beams in which all the material properties were known, Sturm's was found to have the best precision and accuracy.

In the approach of Zhang et al. (2016a,b) the equilibrium of forces is considered to determine the sliding force along a critical diagonal shear crack and shear friction theory is applied to determine the capacity of this shear crack to resist sliding. When this sliding force exceeds the sliding capacity then shear failure occurs and the shear capacity is obtained. Sturm et al. (2020) extended this model to include fibres by including a force perpendicular to the shear crack which is a function of the crack width. The primary issue with this approach was that the numerical implementation was too complex for use in routine design. Hence, in this paper this approach is simplified to produce closed-form solutions where these simplifications represent the novelty in this paper. The resulting solutions are in fact simpler than the current Australian standard as it does not require iteration to determine the longitudinal strain at midspan. This is achieved by approximating the neutral axis depth with the flexural neutral axis depth which is then given by a quadratic equation. This also simplifies the equilibrium equations forming a system of linear simultaneous equations which allowed a simple solution to be derived for the concrete contribution to the shear capacity. The stress in the fibres was also chosen to correspond to the crack width at the effective depth at yield as this provides a simple approach to estimate this value without integrating across a range of crack widths. A closed form solution was also developed for the shear angle which replaces the semi-mechanical expression in Zhang et al. (2016a,b).

The simplified design expressions are validated and compared to existing approaches using tests on 626 reinforced concrete beams without stirrups, 176 reinforced concrete beams with stirrups and 23 FRC beams. From this, the reliability of the proposed expressions was explored. This is important since these expressions give the mean shear strength, however in design, the characteristic shear strength is required. Hence, factors were derived that could be used in conjunction with these expressions to give the characteristic shear strength.

SHEAR CAPACITY OF FIBRE REINFORCED CONCRETE BEAMS

First consider the fundamental mechanics of Sturm et al.’s (2020) model as illustrated in Fig. 1(a) where the forces on the free body on the right hand side A-B-C-D are shown. As the shear force V_u increases, flexural cracks form in the flexural tension region at the bottom face and propagate towards the load point. While tests have shown these cracks to follow a non-linear path, a simplification is applied here in which the non-linear crack is replaced with an equivalent diagonal crack A-B with an angle of β to the horizontal as shown. This simplification is valid as demonstrated by Zhang (1997), Huang & Nielsen (1998), Zhang et al. (2016a;b) and Sturm et al. (2020).

As rotation occurs about this critical shear crack A-B in Fig. 1(a), forces develop in the: tensile reinforcement F_{rt}; compressive concrete F_c; fibres F_f; and in the stirrups F_{st}. In line with the simplifying assumption of Placas & Regan (1971), the compression reinforcement is ignored. In order to maintain equilibrium with the imposed shear force and moment, a force S also occurs along the inclined plane as shown. This sliding force S is resisted along B-C by the concrete in compression and shear failure is considered to occur at the point in which the sliding force S exceeds the shear capacity S_{cap} of the potential sliding plane B-C, at which point a fracture plane extends through the flexural compression region along B-C.

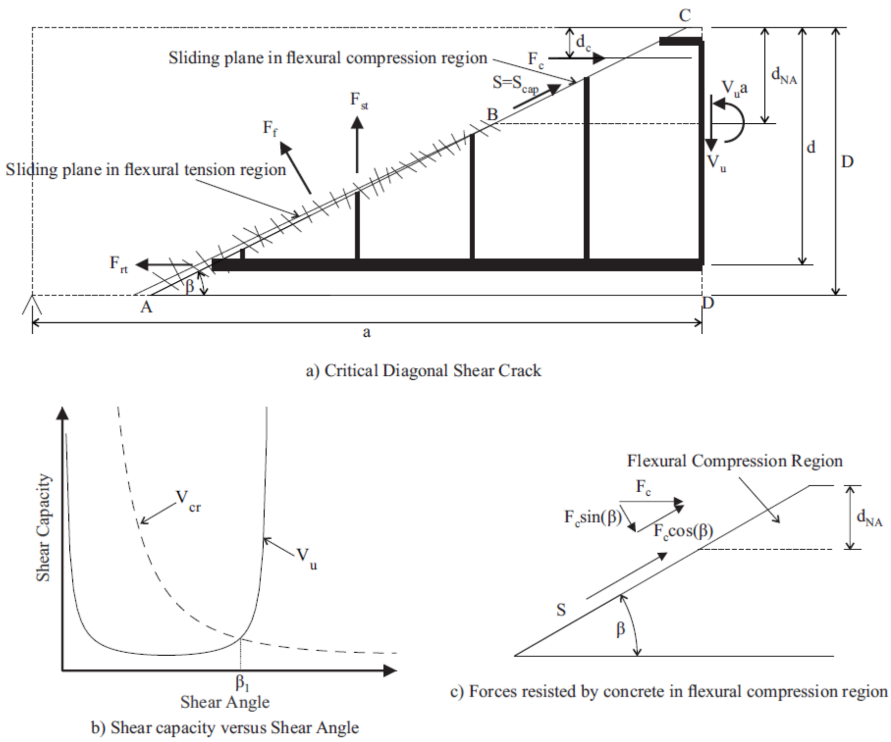

Fig. 1 Mechanics of Shear Failure

The shear stress at the initiation of sliding that is the material shear capacity v can be derived from shear friction theory (Regan & Yu 1973) such that

$$v = m\sigma_N + c \tag{1}$$

where: σ_N is the normal stress which is a function of F_c in Fig. 1(a); m is the frictional component of the shear strength; and c is the cohesion.

The shear strength of the potential sliding plane S_{cap} can be determined by integrating v over this plane in the flexural compression region. Importantly in this approach, the shear capacity is taken as the capacity just prior to the sliding plane extending into the flexural compression region, that is just prior to sliding in the flexural compression region. As once sliding occurs, the material shear capacity reduces (Chen et al. 2015) when σ_N remains the same. Hence, this paper will take the shear capacity as equal to the pre-sliding capacity as this is equal to or a lower bound to the actual shear capacity. This same approach has been adopted by Zhang et al. (2016a;b) and Sturm et al. (2020) where accurate predictions were obtained.

From a numerical analysis (Zhang et al. 2016a; Sturm et al. 2020), it can be shown that the shear capacity V_u, through failure along A-B-C in Fig. 1(a), varies with the inclination of the sliding plane β as shown in Fig. 1(b) (Sturm et al. 2020). However, this failure mode can only occur after the sliding plane A-B in Fig. 1(a) has formed. The shear load to form the sliding plane A-B in Fig. 1(a) has been defined by Zhang (1997) as

$$V_{cr} = \frac{f_{ct}^{*} b D^2}{a \sin^2(\beta)} \tag{2}$$

in which: f_{ct}^* is the effective tensile strength which is equal to $0.6f_{ct}$ where f_{ct} is the concrete tensile strength (Zhang 1997); b is the width of the section; D is the total depth; and a is the shear span.

Consider the variations V_{cr} and V_u in Fig. 1(b). To the right of β_1, V_u exceeds V_{cr} such that the sliding plane forms at V_{cr} before failure at an increased load V_u. To the left of β_1, V_{cr} exceeds V_u such that the sliding plane fails at V_{cr} as the strength then reduces to V_u. Hence the intercept at β_1 governs the ultimate strength.

Having now defined the general mechanics of the approach, now let us consider the mathematical formulation. From vertical equilibrium of the forces illustrated in Fig. 1(a)

$$V_u = S_{cap} \sin(\beta) + F_{st} + F_f \cos(\beta) \tag{3}$$

where F_{st} is the force in the stirrups and F_f is the force in the fibres. For convenience in design, Eq. (3) can be rewritten in the same form as AS3600:2018 (Standards Australia 2018) that is

$$V_u = V_{uc} + V_{us} + V_{uf} \tag{4}$$

in which the contribution of the concrete to the shear capacity is

$$V_{uc} = S_{cap} \sin(\beta) \tag{5}$$

the contribution of the stirrups to the shear capacity is

$$V_{us} = F_{st} \tag{6}$$

and the contribution of the fibres to the shear capacity is

$$V_{uf} = F_f \cos(\beta) \tag{7}$$

Concrete contribution to the shear capacity

The concrete contribution to the shear capacity uses the closed form expression derived by Zhang et al. (2016a) for the shear capacity of reinforced concrete beams without stirrups. From horizontal, vertical and rotational equilibrium

$$0 = F_{rt} - F_c - S_{cap}\cos(\beta) \tag{8}$$

$$V_{uc} = S_{cap}\sin(\beta) \tag{9}$$

$$V_{uc}a = F_{rt}d - F_c d_c \tag{10}$$

where the sliding capacity S_{cap} is obtained by integrating the material shear strength in Eq. (1) over the area of the sliding plane in compression. This sliding capacity is a function of the normal stress due to F_c given by

$$\sigma_N = \frac{F_c\sin(\beta)}{\left[\frac{bd_{NA}}{\sin(\beta)}\right]} = \frac{F_c\sin^2(\beta)}{bd_{NA}} \tag{11}$$

where F_c sin(β) is the component of F_c normal to the sliding plane, whereas, bd_{NA}/sin(β) is the area of the sliding plane in the flexural compression region as illustrated in Fig. 1(c).

The component of F_c parallel to the sliding plane F_c cos(β) in Fig. 1(c) has the corresponding shear stress

$$\tau_N = \frac{F_c\cos(\beta)}{\left[\frac{bd_{NA}}{\sin(\beta)}\right]} = \frac{F_c\sin(\beta)\cos(\beta)}{bd_{NA}} \tag{12}$$

Consequently, the sliding capacity is given by

$$S_{cap} = \int^{\frac{bd_{NA}}{\sin(\beta)}}(v - \tau_N)\,dA = \frac{C_1F_c + cbd_{NA}}{\sin(\beta)} \tag{13}$$

which is the material shear strength less the shear component of F_c.

Substituting Eq. (13) into Eq. (8) and rearranging gives the force in the longitudinal tension reinforcement as

$$F_{rt} = F_c\left[1 + \frac{C_1}{\tan(\beta)}\right] + \frac{cbd_{NA}}{\tan(\beta)} \tag{14}$$

where substituting Eq. (13) into Eq. (9) then rearranging gives the force in the concrete as

$$F_c = \frac{V_{uc} - cbd_{NA}}{C_1} \tag{15}$$

Substituting Eqs. (14) and (15) into Eq. (10) then rearranging gives the shear capacity as

$$V_{uc} = \frac{cbd_{NA}}{C_2} \tag{16}$$

where

$$C_2 = 1 - C_1 \frac{a - \frac{d}{\tan(\beta)}}{d - d_c} \tag{17}$$

in which

$$C_1 = \sin(\beta)\,[m \sin(\beta) - \cos(\beta)] \tag{18}$$

where d is the effective depth, d_{NA} is the neutral axis depth and d_c is the lever arm of the concrete.

The primary differences between the above solution and that in Sturm et al. (2020) are the unknown variables when solving Eqs. (8-10). In the numerical model, the unknown variables were the shear capacity V_{uc}, the rotation θ and the neutral axis depth d_{NA}. However, in the solution presented here, d_{NA} is approximated using its value at flexure. This has allowed the replacement of θ and d_{NA} by F_{rt} and F_c. This simplifies the solution, as the solution in Sturm et al. (2020) had terms that were products of θ and d_{NA} which resulted in the neutral axis depth d_{NA} having to be determined from a quartic equation for the non-iterative solution. In this case, there are no terms that are products of F_{rt} and F_c, hence, Eqs. (8-10) form a system of linear simultaneous equations which are straightforward to solve. This change in unknowns also means that the stress-strain relationship of the concrete or the load-slip relationship of the reinforcement is not required in the solution further reducing complexity.

Neutral axis depth

To solve Eq. 18, the neutral axis depth can be approximated using the flexural cracked neutral axis (Zhang et al. 2016a). For an FRC beam this is complicated by the fact the cracked neutral axis depth varies with the applied moment and is not a constant (Sturm et al. 2019). Hence, as a lower bound on the neutral axis depth the value at the yield of the longitudinal reinforcement can be used. At yield the force in the reinforcement is given by

$$F_{rt} = E_r A_{rt} \chi (d - d_{NA}) = f_y A_{rt} \tag{19}$$

where E_r is the elastic modulus of the reinforcement, A_{rt} is the cross-sectional area of the tensile reinforcement, χ is the curvature, d is the effective depth, d_{NA} is the neutral axis depth and f_y is the yield strength of the reinforcement. Hence rearranging Eq. (19) gives the curvature as

$$\chi = \frac{f_y}{E_r(d - d_{NA})} \tag{20}$$

The force in the fibres is then given by

$$F_f = f_f b (D - d_{NA}) \tag{21}$$

where f_f is the stress in the fibres, b is the width of the section and D is the total depth. The force in the concrete is given by

$$F_c = \frac{1}{2} b d_{NA}^2 E_c \chi \tag{22}$$

where E_c is the elastic modulus of the concrete.

Hence from horizontal equilibrium

$$0 = F_{rt} + F_f - F_c = f_y A_{rt}(d - d_{NA}) + f_f b (h - d_{NA})(d - d_{NA}) - \frac{1}{2} b d_{NA}^2 E_c \frac{f_y}{E_r} \tag{23}$$

The solution to Eq. (23) is given by

$$d_{NA} = d\left(\frac{a_2 - \sqrt{a_2^2 - 4a_1 a_3}}{2a_1}\right) \tag{24}$$

where

$$a_1 = -\frac{1}{2n} + \frac{f_f}{f_y} \tag{25}$$

$$a_2 = \rho + \frac{f_f}{f_y}\left(1 + \frac{D}{d}\right) \tag{26}$$

$$a_3 = \rho + \frac{f_f}{f_y}\frac{D}{d} \tag{27}$$

in which ρ is the reinforcement ratio, *n* is the modular ratio, f_f is the fibre stress, f_y is the yield stress and *D* is the total depth. Note that if f_f is set to zero the neutral axis depth for a section without fibres is obtained. The lever arm of the concrete is given by $d_{NA}/3$ (Zhang et al. 2016a).

Shear Angle

The development of a fully closed form solution for the shear angle is the primary change from that presented in Zhang et al. (2016a) which used a semi-mechanical expression based on a numerical model. A further benefit of this closed form solution is that it can incorporate new materials, whereas, the semi-mechanical expressions need to be recalibrated. From Fig. 1(b) the shear angle is given when the sliding capacity given by Eq. (16) is equal to the shear force to cause diagonal cracking given by Eq. (2). Rearranging this gives the following equation for β_1

$$0 = 1 - \sin^2(\beta_1)\left(\frac{ma}{d-d_c} + C_3\right) + \sin(\beta_1)\cos(\beta_1)\frac{md+a}{d-d_c} - \cos^2(\beta_1)\frac{d}{d-d_c} \tag{28}$$

where

$$C_3 = \frac{cad_{NA}}{f_{ct}^{*}D^2} \tag{29}$$

Applying trigonometric identities (Olver et al. 2010)

$$\sin(\beta)\cos(\beta) = \frac{\tan(\beta)}{1+\tan^2(\beta)} \tag{30}$$

$$\sin^2(\beta) = \frac{1}{2} - \frac{1}{2}\left[\frac{1-\tan^2(\beta)}{1+\tan^2(\beta)}\right] \tag{31}$$

$$\cos^2(\beta) = \frac{1}{2} + \frac{1}{2}\left[\frac{1-\tan^2(\beta)}{1+\tan^2(\beta)}\right] \tag{32}$$

and rearranging gives

$$0 = b_1\tan^2(\beta_1) + b_2\tan(\beta_1) + b_3 \tag{33}$$

where

$$b_1 = 1 - \frac{ma}{d-d_c} - C_3 \tag{34}$$

$$b_2 = \frac{md+a}{d-d_c} \tag{35}$$

$$b_3 = 1 - \frac{d}{d-d_c} \tag{36}$$

Hence the shear angle is given by

$$\beta_1 = \arctan\left(\frac{-b_2 - \sqrt{b_2^2 - 4b_1 b_3}}{2b_1}\right) \tag{37}$$

Stirrup contribution to the shear capacity

In Zhang et al. (2016b) and Sturm et al. (2020), the contribution of the stirrups to the shear capacity was determined by evaluating the force in each individual stirrup as a function of the vertical opening of the shear crack. This crack opening is a function of the neutral axis depth d_{NA} and rotation. This approach is not applicable to our simplified solution as the rotation is never determined. For the closed-form solution in Zhang et al. (2016b), this issue was mitigated by relating the force in the stirrups to the force in the reinforcement. The solution, however, is still not ideal for design as there is uncertainty about whether the stirrups have or have not yielded. To resolve this problem, Zhang's solution required the shear capacity to be determined assuming the stirrups are elastic then checking whether the stirrups should have yielded. If some of the stirrups should have yielded, the shear capacity would be assessed using the correct assumption. Another problem is that the exact position of the stirrups with respect to the shear crack is not known.

To overcome the above uncertainties and to simplify the problem, the conventional solution of smeared and yielded stirrups was adopted. The force in the stirrups in Fig. 1(a) is given by

$$V_{us} = f_y \frac{A_{rv}}{s} \frac{d - d_{NA}}{\tan(\beta)} \quad (38)$$

where A_{rv} is the area of transverse reinforcement and s is the spacing. This assumption can appear to be unconservative because, as shown by the numerical analyses conducted by Zhang et al. (2016b) and the experimental work of Wu & Hu (2017), rarely are all the stirrups yielded in practice at the onset of shear failure. This is mitigated by the fact that while Eq. (42) overstates the direct contribution of the stirrups to the shear capacity, the increase in the force in the concrete F_c due to the stirrups (Zhang et al. 2016b) was not included in the derivation of V_{uc}. To determine whether this is correct, a large number of beams with stirrups based on the beams used in the ensuing validation, was analysed using both the above smeared approach and the discrete crack model presented in Zhang et al. (2016b). The results are shown in Fig. 2, where it is observed that the results from the smeared and discrete approaches are generally similar. The safety of this approximation is also established in the validation.

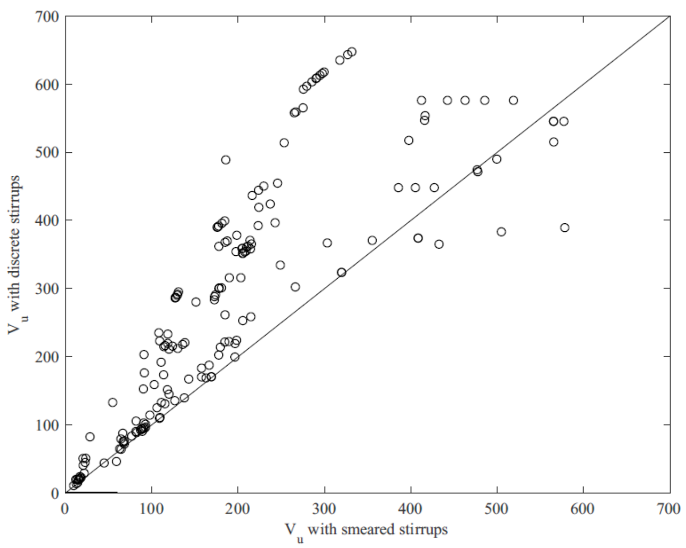

Fig. 2 Comparison of smeared and discrete stirrup models

Fibre contribution to the shear capacity

The force in the fibres F_f in Fig. 1(a) is given by integrating the stress in the fibres over the area of the sliding plane that is in tension

$$F_f = \int^{\frac{b(h-d_{NA})}{\sin(\beta)}} \sigma_f(w)dA = f_f \frac{b(D-d_{NA})}{\sin(\beta)} \tag{39}$$

where $\sigma_f(w)$ is the stress in the fibres as a function of the crack width w and f_f is the average fibres stress that is constant over the depth. The resulting fibre contribution to the shear capacity is given by

$$V_{uf} = f_f \frac{b(D-d_{NA})}{\tan(\beta)} \tag{40}$$

The fibre stress f_f depends on both the magnitude and variation of the crack width along the tensile region of the sliding plane, as given by the empirical tensile stress-crack width relationship which is a material property. This can be assessed either directly using tension tests or indirectly using flexural tests with an associated inverse analysis. In general, the fibre stress reduces with increasing crack width. A result of this is that the stress is maximum near the tip of the crack and a minimum at the bottom fibre. Hence to achieve a simple and conservative solution, the fibre stress is chosen to correspond to the crack width at the depth of the tensile reinforcement which is close to the bottom fibre of the section. Furthermore, to provide an upper bound to the crack width and, therefore, a lower bound to f_f, the reinforcement strain is set to the yield strain ε_y so that the crack width can be approximated as

$$w_d = \varepsilon_y S_{cr} \tag{41}$$

where S_{cr} is the crack spacing which can be determined using the following expression from Sturm et al. (2018)

$$S_{cr} = \left[\frac{2^{\alpha}(1+\alpha)}{\lambda_2(1-\alpha)^{1+\alpha}}\right]^{\frac{1}{1+\alpha}} \left[\frac{f_{ct}-f_{pc}}{E_c}\left(\frac{E_c A_{ct}}{E_r A_{rt}}+1\right)\right]^{\frac{1-\alpha}{1+\alpha}} \tag{42}$$

in which

$$\lambda_2 = \frac{\tau_{max} L_{per}}{\delta_1^{\alpha}}\left(\frac{1}{E_c A_{ct}} + \frac{1}{E_r A_{rt}}\right) \tag{43}$$

where τ_{max} is the maximum bond stress for the longitudinal reinforcement, δ_1 is the slip at the maximum bond stress for the longitudinal reinforcement, α is the non-linearity, L_{per} is the bonded perimeter, A_{rt} is the cross-sectional area of tensile reinforcement, A_{ct} is the cross-sectional area of the tension chord, E_c is the elastic modulus of the concrete and f_{pc} is the post-cracking stress. The bond parameters τ_{max}, δ_1 and α can be identified from the bond stress-slip relationship of the longitudinal reinforcement is determined from pullout tests on embedded reinforcement as shown in Fig. 3(a). Where experimental data is unavailable, the expressions suggested by Harajli (2009) for FRCs with strengths less than 100 MPa and Sturm & Visintin (2018) for FRCs with strengths exceeding 100 MPa can be used. The geometry of the tension chord is illustrated in Fig. 3(b) as this defines L_{per} and $A_{ct.}$ The post-cracking stress can be estimated as the first local minimum after the peak as was done in Sturm et al. (2018)

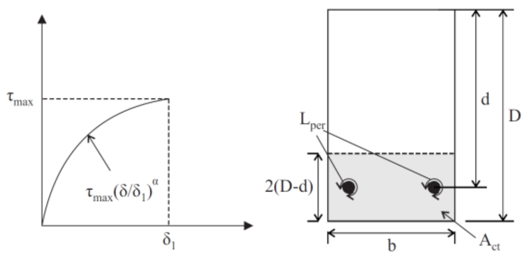

a) Bond stress-slip relationship b) Geometry of Tension Chord

Fig. 3 Bond stress-slip relationship and geometry of tension chord

To use the crack width from Eq. (41), the tensile stress-crack width relationship is required. As there are no general material models that cover the full range of FRC mixes, this needs to be determined experimentally. There has been little uniformity in terms of the testing approaches applied to FRC to characterise the tensile response. In the opinion of the authors, the best approach is to measure this directly using specimens sufficiently large such that the 3D orientation of the fibres is not disturbed such as those suggested by AS3600:2018 (Standards Australia 2018) or Visintin et al. (2018). Specimens that are not sufficiently large may disturb the distribution of the fibres such that they become aligned with the applied force, hence, overestimating the tensile strength for members where this is not the case.

VALIDATION

Reinforced concrete members without stirrups

The shear capacity expressions proposed in this paper for reinforced concrete members without stirrups are first validated against a database of 626 tests from 26 references (Moody et al. 1954; Morrow & Viest 1957; Chang & Kesler 1958; Watstein & Mathey 1958; Sozen et al. 1959; Diaz de Cossio & Siess 1960; Diaz de Cossio 1962; Leonhardt & Walther 1962; Bresler & Scordelis 1963; Mathey & Watstein 1963; Kani 1966; Krefeld & Thurston 1966; Kani 1967; Bhal 1968; Mattock 1969; Placas & Regan 1971; Taylor 1972; Walraven 1978; Chana 1981; Mphonde & Frantz 1984; Kotsovos 1987; Papadakis 1996; Collins & Kuchma 1999; Kim & White 1999; Yost et al. 2001; Tang et al. 2009) compiled by Zhang et al (2016). The details of the tests used for the validation are summarised in a spreadsheet in the supplementary material. The tests are compared in Fig. 4 to the procedure in this paper as well as the codified approaches in AS3600:2018 (Standards Australia 2018), ACI 318-19 (ACI 2019) and in Eurocode 2 (CEN 2004). For the validation, the elastic modulus of the reinforcement was assumed to be 200 GPa while the elastic modulus of the concrete and the tensile strength where estimated using the expressions in the fib Model Code 2010 (fib 2013). The shear friction material properties suggested by Zhang et al. (2014b) were used in this validation.

$$m = \frac{0.389 f_c - c}{0.250\, f_c} \tag{44}$$

$$c = 1.15 f_{ct} \tag{45}$$

where f_c is the concrete compressive strength and f_{ct} the tensile strength.

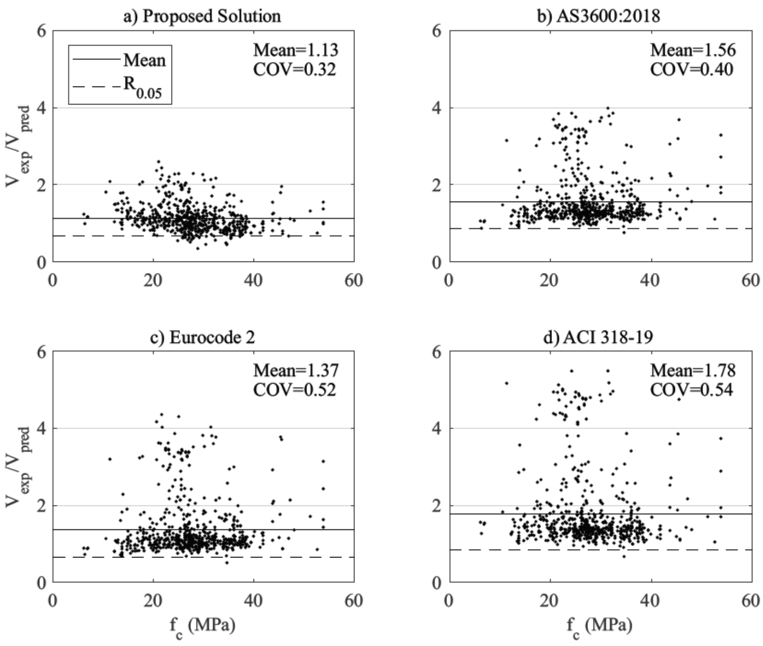

Fig. 4 Validation for reinforced concrete beams without stirrups

It can be seen in Fig. 4 that the proposed approach has a coefficient of variation (COV) of 0.32 which is a significant improvement over the codified approaches where the COV ranges from 0.40 to 0.54, also shown in Fig. 4, the mean fit of the proposed approach is 1.13 compared to the range of 1.37 to 1.78 for the existing approaches. For design, the characteristic shear capacity is

$$V_d = 0.66V_{uc} \tag{46}$$

which was estimated by fitting a lognormal distribution. The characteristic value is given by the lognormal distribution as

$$R_{0.05} = \exp(\lambda - 1.645\varepsilon) \tag{47}$$

where λ is the mean of log(*x*), ε is the standard deviation of log(*x*) and *x* is the ratio of the experimental to predicted values; this is derived in Appendix A.

Reinforced concrete members with stirrups

The shear capacity expressions for reinforced concrete members with stirrups are validated against a database of 176 tests from 16 references (Clark 1951; Bresler & Scordelis 1963; Krefeld & Thurston 1966; Placas & Regan 1971; Swamy & Andriopoulos 1974; Mattock & Wang 1984; Mphonde & Frantz 1985; Elzanaty et al. 1986; Anderson & Ramirez 1989; Sarsam & Al-Musawi 1992; Xie et al. 1994; Yoon et al. 1996; Frosch 2000; Tompos & Frosch 2002; Lee & Hwang 2010; Lee et al. 2011) compiled by Zhang et al. (2016b). The results are compared in Fig. 5 to the procedure in this paper as well as the codified approaches AS3600:2018 (Standards Australia 2018), ACI 318-19 (ACI 2019) and Eurocode 2 (CEN 2004). The proposed approach has the best COV of 0.22 which is a minor improvement over the codified approaches that range between a COV of 0.23 and 0.36. However, the better fit to beams without stirrups and to FRC beams generally validates this approach. It should be noted that the presented approach is conservative with a mean of 1.4 which is in the same range as for the codified approach which is due to using a smeared rather than discrete approach for the stirrups. Hence the design shear capacity in this case is given by

$$V_d = 0.95(V_{uc} + V_{us}) \tag{48}$$

For the validation, the elastic modulus of the reinforcement was again assumed to be 200 GPa while the elastic modulus and tensile strength of the concrete were estimated with the expressions in the fib Model Code 2010 (fib 2013). Eqs. (44) and (45) were again used to determine the shear friction material properties.

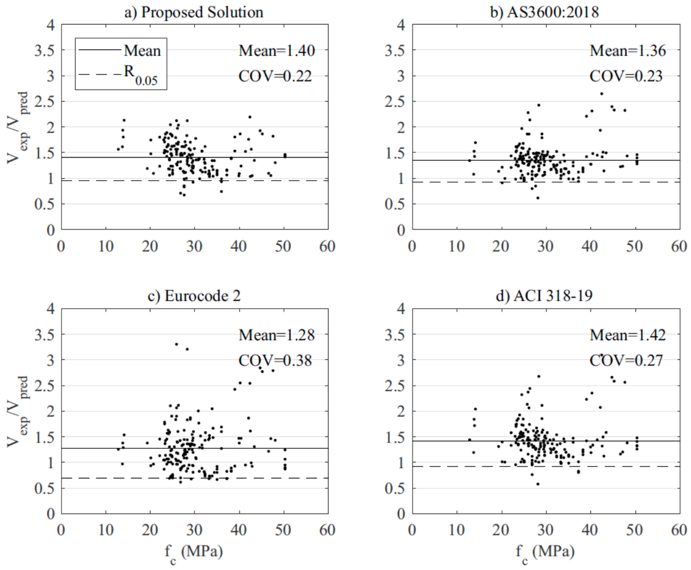

Fig. 5 Validation for reinforced concrete beams with stirrups

FRC members without stirrups

The shear capacity of FRC members is validated against a database of 23 tests from 3 references (Casanova et al. 1997; Noghabai 2000; Amin & Foster 2016) compiled by Sturm et al. (2020). There have been a large number of shear tests performed on FRC beams as evidenced by Lantsoght (2019), however in general, the tensile response of the FRC was poorly characterised which makes comparison difficult. Hence, the data was only chosen from tests where the tensile response was characterised over a range of crack widths in direct tension. The tests are compared in Fig. 6 to the proposed approach as well as the solutions in Sturm et al. (2020)[a], Sturm et al. (2020)[b], AS3600:2018 (Standards Australia 2018), AFGC (2013) and fib Model Code 2010 (fib 2012), Choi et al. (2007), Zhang et al, (2016c) and Lee et al. (2016); "Sturm et al. (2020)[a]" refers to a numerical solution and "Sturm et al. (2020)[b]" refers to the non-iterative solution. Additionally, "fib Model Code 2010[a]" refers to the solution based on the Eurocode 2 shear capacity expression while "fib Model Code 2010[b]" refers to the shear capacity expression based on simplified modified compression field theory. Note that the shear friction material properties were estimated again using Eqs. (44) and (45).

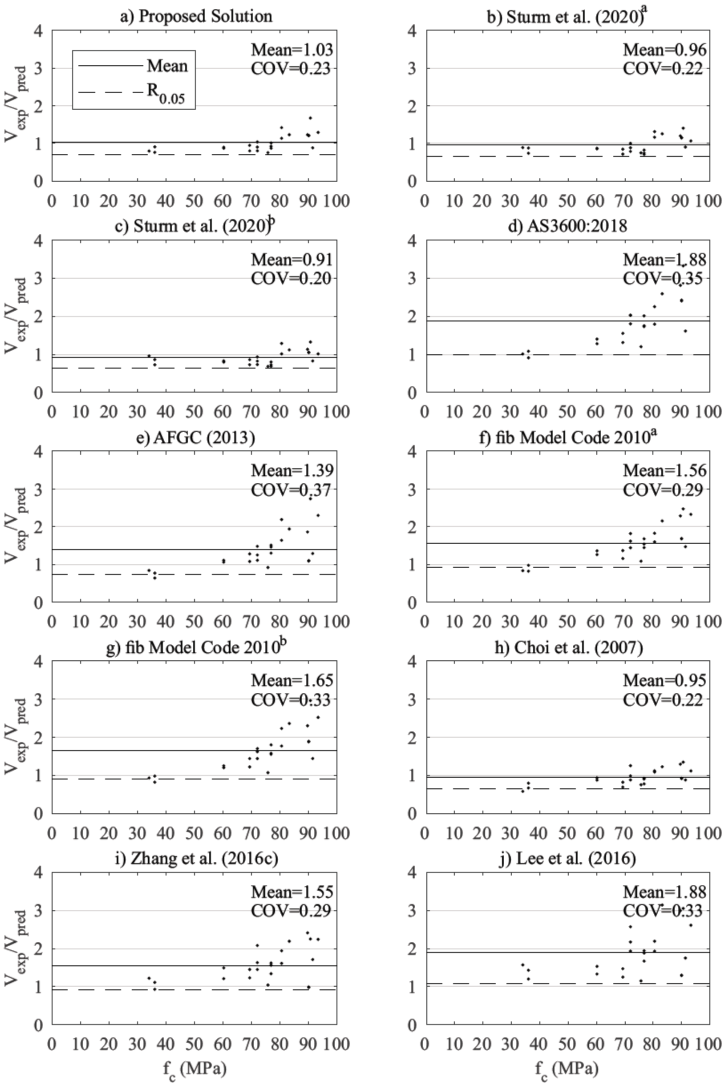

Fig. 6 Validation for FRC beams

From the comparisons in Fig. 6, the proposed solution was found to have a COV of 0.23 which can be compared to a COV of 0.20-0.22 for the approaches proposed in Sturm et al. (2020). Hence, the significant simplifications in this paper have only produced a minimal loss in accuracy. The COV of 0.23 is also a significant improvement on the codified approaches which had COVs between 0.29 and 0.37. The codified approaches are also conservative with means between 1.39 and 1.88 as compared to the 1.03 for the proposed solution. Zhang et al. (2016c) and Lee et al. (2016) had means and COVs in the same range as the codified approaches. However, the mean and COV for Choi et al. (2007) is in the same range as the proposed solution. This is interesting as they propose a similar shear failure mechanism to Sturm et al. (2020) where the shear failure is controlled by the shear crack penetrating the flexural compression region. The proposed solution however is simpler than that proposed by Choi et al. (2007) since it does not require iteration to determine the maximum compressive strain at the loading point. The design shear capacity in this case is given by

$$V_d = 0.70\left(V_{uc} + V_{uf}\right) \tag{49}$$

FRC members with stirrups

Further avenues for research include FRC beams with stirrups as it would be useful to determine the reliability of these expressions when applied in this case. This was not done in this study as the only study available in the literature where the tensile response was well characterised was performed by Amin & Foster (2016), hence, sufficient data to determine the reliability of these expressions is not available.

ANALYSIS WORKED EXAMPLE

Consider the FRC beam in Fig. 7.

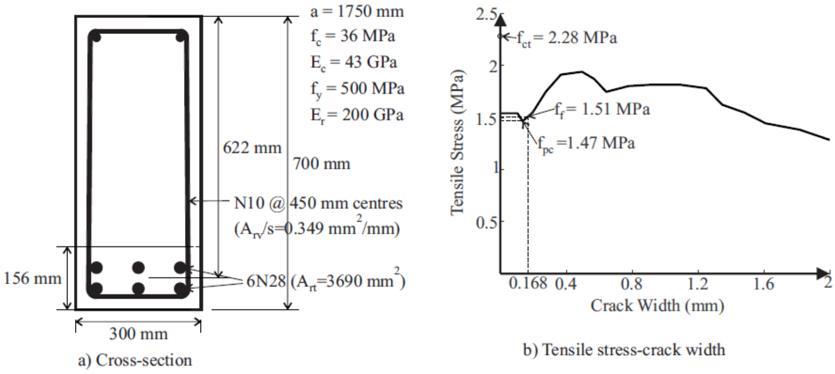

Fig. 7 Analysis worked example

The first step is to estimate the crack spacing, so starting with the bond parameter from Eq. (43)

$$\lambda_2 = \frac{(15.4\,MPa)(528\,mm^2)}{(1.5\,mm)^{0.3}}\left[\frac{1}{(43000\,MPa)(46800\,mm^2)} + \frac{1}{(200000\,MPa)(3690\,mm^2)}\right] = 13.3 \times 10^{-6}\,mm^{-0.3} \quad (50)$$

where τ_{max} is 15.4 MPa, δ_1 is 1.5 mm, α is 0.3 using the expressions in Harajli (2009). Furthermore, A_{ct} is 46800 mm^2 and L_{per} is 528 mm^2. Hence the crack spacing is given by Eq. (42) as

$$S_{cr} = \left[\frac{2^{0.3}(1.3)}{(13.3\times10^{-6}\,mm^{-0.3})(0.7)^{1,3}}\right]^{\frac{1}{1.3}}\left[\frac{2.28\,MPa - 1.47\,MPa}{43000\,MPa}\left(\frac{(43000\,MPa)(46800\,mm^2)}{(200000\,MPa)(3690\,mm^2)} + 1\right)\right]^{\frac{0.7}{1.3}} = 67.0\,mm \quad (51)$$

The crack width at the depth of the tensile reinforcement is given by Eq. (41) using the yield strain 0.0025

$$w_d = 0.0025(42.0\,mm) = 0.168\,mm \quad (52)$$

Hence, the fibre stress f_f is 1.51 MPa. The next step is to evaluate the neutral axis depth. From Eqs. (25-27)

$$a_1 = -\frac{1}{2(4.65)} + \frac{1.51\,MPa}{500\,MPa} = -0.105 \quad (53)$$

$$a_2 = 0.0198 + \frac{1.51\,MPa}{500\,MPa}\left(1 + \frac{700\,mm}{622\,mm}\right) = 0.0262 \quad (54)$$

$$a_3 = 0.0198 + \frac{1.51\,MPa}{500\,MPa}\frac{700\,mm}{622\,mm} = 0.0232 \quad (55)$$

where the modular ratio n is 4.65 and the reinforcement ratio is ρ is 0.0198. Substituting in Eqs. (25-27) into Eq. (24)

$$\frac{d_{NA}}{d} = \frac{0.0262 - \sqrt{(0.0262)^2 + 4(0.105)(0.0232)}}{-2(0.105)} = 0.362 \quad (56)$$

Hence, the neutral axis depth d_{NA} is 225 mm such that the lever arm of the concrete d_c is 75 mm. The shear friction material properties can be estimated using Eqs. (44-45) to give m of 1.26 and c of 2.62 MPa. The next step is to evaluate the shear angle. Thus from Eq. (29)

$$C_3 = \frac{(2.62MPa)(1750\ mm)(225\ mm)}{(1.37\ MPa)(700\ mm)^2} = 1.54 \tag{57}$$

where the effective tensile strength f_{ct}* is 1.37 MPa. From Eq. (34-36)

$$b_1 = 1 - \frac{(1.26)(1750\ mm)}{622\ mm - 75\ mm} - 1.54 = -4.57 \tag{58}$$

$$b_2 = \frac{(1.26)(622\ mm) + 1750mm}{622\ mm - 75\ mm} = 4.63 \tag{59}$$

$$b_3 = 1 - \frac{622\ mm}{622\ mm - 75\ mm} = -0.137 \tag{60}$$

Hence the shear angle is given by Eq. (37).

$$\tan(\beta_1) = \frac{-4.63 - \sqrt{(4.63)^2 - 4(4.57)(0.137)}}{-2(4.57)} = 0.983 \tag{61}$$

Therefore, the shear angle β_1 is given as 0.777 radians or 44.5°. The shear contribution due to the concrete can now be evaluated. Hence, from Eqs. (16-18)

$$C_1 = \sin(0.777)\,[1.26\ \sin(0.777) - \cos(0.777)] = 0.120 \tag{62}$$

$$C_2 = 1 - 0.120\,\frac{1750\ mm - \frac{622\ mm}{0.983}}{622\ mm - 75\ mm} = 0.755 \tag{63}$$

$$V_{uc} = \frac{(2.62\ MPa)(300\ mm)(225\ mm)}{0.755} = 234kN \tag{64}$$

The contribution of the stirrups is given by Eq. (38)

$$V_{us} = (500\ MPa)\left(0.349\,\frac{mm^2}{mm}\right)\frac{622\ mm - 225\ mm}{0.983} = 70.5\ kN \tag{65}$$

The contribution of the fibres is given by Eq. (40)

$$V_{uf} = (1.51\ MPa)\,\frac{(300\ mm)(700\ mm - 225\ mm)}{0.983} = 219\ kN \tag{66}$$

Hence the shear capacity is given by Eq. (4) as

$$V_u = 234\ kN + 70.5\ kN + 219\ kN = 524\ kN \tag{67}$$

DESIGN WORKED EXAMPLE

Consider the beam in Fig. 8.

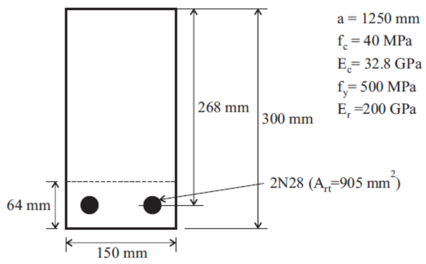

Fig. 8 Design worked example

The beam is subject to as shear force *V** of 100 kN. So first determine the shear capacity of the section without fibres or stirrups. From Eqs. (44-45) the shear friction material properties are *m* equal to 1.29 and *c* equal to 2.62 MPa. Next evaluate the neutral axis depth. So, first evaluate Eqs. (25-27)

$$a_1 = -\frac{1}{2(6.1)} = -0.082 \quad (68)$$

$$a_2 = a_3 = \rho = 0.0225 \quad (69)$$

where the modular ratio *n* is 6.1 and the reinforcement ratio ρ is 0.0225. From Eq. (24) the neutral axis depth is

$$\frac{d_{NA}}{d} = \frac{0.0225 - \sqrt{(0.0225)^2 + 4(0.082)(0.0225)}}{-2(0.082)} = 0.404 \quad (70)$$

Hence the neutral axis depth d_{NA} is 108 mm. The lever arm of the concrete d_c is 36 mm. Next evaluate the shear angle. Hence from Eq. (29)

$$C_3 = \frac{(2.62\, MPa)(1250\, mm)(108\, mm)}{(1.37\, MPa)(300\, mm)^2} = 2.87 \quad (71)$$

Next evaluate Eqs. (34-36)

$$b_1 = 1 - \frac{(1.29)(1250\, mm)}{268\, mm - 36\, mm} - 2.87 = -8.82 \quad (72)$$

$$b_2 = \frac{(1.29)(268\, mm) + 1250 mm}{268\, mm - 36\, mm} = 6.88 \quad (73)$$

$$b_3 = 1 - \frac{268\, mm}{268\, mm - 36\, mm} = -0.155 \quad (74)$$

Hence the shear angle is given by Eq. (37) as

$$\tan(\beta_1) = \frac{-6.88 - \sqrt{6.88^2 - 4(8.82)(0.155)}}{-2(8.82)} = 0.757 \tag{75}$$

Therefore, the shear angle is 0.648 radians or 37.1°. The shear contribution of the concrete is now given by Eqs. (16-18) as

$$C_1 = \sin(0.648)\,[1.29\sin(0.648) - \cos(0.648)] = -0.0113 \tag{76}$$

$$C_2 = 1 + 0.0113\,\frac{1250\,mm - \frac{268\,mm}{0.757}}{268\,mm - 36\,mm} = 1.04 \tag{77}$$

$$V_{uc} = \frac{(2.62\,MPa)(150\,mm)(108\,mm)}{1.04} = 40.8\,kN \tag{78}$$

Hence, if the total required shear capacity is 100 kN then an additional 59.2 kN is required from the fibres. Hence rearranging Eq. (40) gives the required stress in the fibres as

$$f_f = \frac{V_{uf}}{b(D-d_{NA})}\tan(\beta) = \frac{59200\,N}{(150\,mm)(300\,mm-108\,mm)}0.757 = 1.56\,MPa \tag{79}$$

Note that the presence of fibres effects the neutral axis depth. Recalculating the neutral axis depth using this fibre stress gives the neutral axis depth as 112 mm. Using the new value of the neutral axis depth the shear angle is 36.8° and the concrete contribution to the shear capacity is 41.1 kN. Using these new values the required fibre stress is again 1.56 MPa.

The next step is to determine the crack width at which this stress needs to occur. So from Eqs. (50-51) the crack spacing is given by

$$\lambda_2 = \frac{(16.3\,MPa)(151\,mm^2)}{(1.5\,mm)^{0,3}}\left[\frac{1}{(32800\,MPa)(9600\,mm^2)} + \frac{1}{(200000\,MPa)(905\,mm^2)}\right] = 19\times10^{-6}mm^{-0.3} \tag{80}$$

$$S_{cr} = \left[\frac{2^{0.3}(1.3)}{(19\times10^{-6}\,mm^{-0.3})\,(0.7)^{1.3}}\right]^{\frac{1}{1.3}}\left\{\frac{2.28\,MPa-1.56\,MPa}{32800\,MPa}\left[\frac{(32800\,MPa)(9600\,mm^2)}{(200000\,MPa)(905\,mm^2)}+1\right]\right\}^{\frac{0.7}{1,3}} = 46.9mm \tag{81}$$

in which τ_{max} is 16.3 MPa, δ_1 is 1.5 mm and α is 0.3 using the expressions in Harajli (2009). From the geometry of the tension chord in Fig. 3(b) L_{per} is 151 mm and A_{ct} is 9600 mm^2. Hence, from Eq. (41) the crack width is given by

$$w_d = 0.0025(46.9\,mm) = 0.117\,mm \tag{82}$$

Therefore, FRC with a minimum tensile stress of 1.56 MPa at a crack width of 0.117 mm can be used.

If the required shear capacity was actually 150 kN then this 50 kN shortfall could be accommodated by including transverse reinforcement, hence rearranging Eq. (38) gives

$$\frac{A_{rv}}{s} = \frac{V_{us}}{f_y(d-d_{NA})}\tan(\beta) = \frac{50000\ N}{500\ MPa(268\ mm-112\ mm)}(0.874) = 0.56\ mm^2/mm \qquad (83)$$

where the yield strength of the transverse reinforcement is 500 MPa. Hence, this requirement can be met by providing 8 mm diameter stirrups at 150 mm spacings.

CONCLUSION

Based on free body mechanics, simple design rules have been developed for the shear capacity of reinforced concrete beams. It has been demonstrated from the validation that these solutions are more accurate and precise than conventionally codified solutions for reinforced concrete beams without stirrups and FRC beams while providing comparable performance to the conventional codified solutions for reinforced concrete beams with stirrups. These rules separate the contributions of the concrete, stirrups and fibres to the shear capacity and as such can be used by engineers as a convenient tool to design members with any combination of concrete, stirrups and fibres and with new types of materials. To illustrate the convenience of this approach, a worked example of a design is given.

Previous studies have demonstrated that the application of mechanics can result in accurate solutions for the shear capacity of FRC beams. However, these solutions were too complicated for design. Hence in this paper, new design oriented solutions have been developed for the shear capacity of FRC beams. The simplifications that were applied include using the flexural neutral axis depth which removes the need to iterate this parameter. In this case the equations for equilibrium form a system of linear equations which have a simple solution. A closed-form solution for the shear angle was also developed. A convenient approach has also been suggested for estimating the stress in the fibres without having to integrate the values across a range of crack widths. These have then been validated and compared to codified solutions where it was found that for reinforced concrete beams without stirrups the COV was 0.32 compared to 0.40 for the best codified solution. The mean was also 1.13 as compared to 1.56 for the best codified solution. For reinforced concrete beams with stirrups, the COV was 0.22 compared to 0.23 for the best codified solution. The mean was 1.4 which is in the same range as for the other solutions. For FRC beams, the COV was 0.23 compared to 0.35 for the current Australian standard. The mean was 1.03 as compared to 1.88 for the current Australian standard. The solution also retains much of the accuracy of the numerical solutions presented in Sturm et al. (2020) with the COV increasing to only 0.23 from a COV of 0.20. The presented solutions are also simpler than the current Australian standard as no iteration is required to determine the longitudinal strain at the centroid of the beam. Additionally, a log-normal distribution was fitted to the experimental to predicted results to allow the characteristic shear strength to be determined from the mean values. The primary improvement over previous codified expressions for shear is that the concrete and fibre contributions are related to the neutral axis depth. The solution also includes a simple method to estimate the fibre stress which does not require either the use of an excessively conservative value or iteration to determine the fibre stress.

APPENDIX A CHARACTERISTIC RESISTANCE FOR LOG-NORMAL DISTRIBUTION

The characteristic value is defined as the value for which only 5% of observations are less than the given value. The cumulative distribution function for a log-normal distribution (Melchers & Beck 2018) is

$$F(x) = \Phi\left[\frac{\ln(x)-\lambda}{\varepsilon}\right] \quad \text{(A1)}$$

where x is the random variable, $\Phi(x)$ is the cumulative distribution function for a normal distribution, λ is the mean of log(x) and ε is the standard deviation of log(x). Hence setting $F(x)$ to 0.05 gives

$$\frac{\ln(R_{0.05})-\lambda}{\varepsilon} = \Phi^{-1}(0.05) = -1.645 \quad \text{(A2)}$$

where $R_{0.05}$ is the characteristic value and $\Phi^{-1}(x)$ is the inverse cumulative distribution function for a normal distribution. Rearranging gives the characteristic value as

$$R_{0.05} = \exp(\lambda - 1.645\varepsilon) \quad \text{(A3)}$$

DATA AVAILABILITY STATEMENT

All data, models, and code generated or used during the study appear in the submitted article.

ACKNOWLEDGEMENTS

This material is based upon work supported by the Australian Research Council Discovery Project 190102650"

NOTATION

A_{ct} = cross-sectional area of tension chord;

A_{rt} = cross-sectional area of tensile reinforcement;

A_{rv} = cross-sectional area of stirrups;

a = shear span;

a_1, a_2, a_3 = parameters for Eq. (24)

b = width;

b_1, b_2, b_3 = parameters for Eq. (33);

C_1, C_2 = parameters for Eq. (16);

C_3 = parameter for Eq. (34);

c = cohesive component of the shear strength;

D = total depth;

d = effective depth;

d_c = lever arm of the compressive concrete;

d_{NA} = neutral axis depth;

E_c = elastic modulus of the concrete;

E_r = elastic modulus of the reinforcement;

$F(x)$ = cumulative distribution function for log-normal distribution;

F_c = force in the compressive concrete;

F_f = force in the fibres;

F_{rt} = force in tensile reinforcement;

F_{st} = force in the stirrups;

f_c = concrete strength;

f_{ct} = tensile strength;

f_{ct}^* = effective tensile strength;

f_f = stress in the fibres;

f_{pc} = post cracking stress;

f_y = yield strength;

L_{per} = bonded perimeter;

m = frictional component of the shear strength;

n = modular ratio ($=E_r/E_c$);

$R_{0.05}$ = characteristic value;

S_{cap} = sliding capacity;

S_{cr} = crack spacing;

s = stirrup spacing;

V_{cr} = shear force to cause cracking;

V_d = design shear capacity;

V_u = mean shear capacity;

V_{uc} = contribution of the concrete to the shear capacity;

V_{uf} = contribution of the fibres to the shear capacity;

V_{us} = contribution of the stirrups to the shear capacity;

v = material shear strength;

w_d = crack width at the effective depth;

x = random variable;

α = non-linearity;

β = shear angle;

β_1 = angle of critical diagonal shear crack;

δ_1 = slip at the maximum bond stress;

ε = standard deviation of log(x);

ε_d = strain at the effective depth;

θ = rotation;

λ = mean of log(x);

λ_2 = bond parameter;

ρ = reinforcement ratio ($=A_{rt}/bd$);

σ_N = normal stress;

τ_max = maximum bond stress;

$\Phi(\mathrm{x})$ = cumulative distribution function for normal distribution;

χ = curvature;

REFERENCES

ACI (American Concrete Institute) (2019). "Building Code Requirements for Structural Concrete." *ACI 318-19*, Farmington Hills.

AFGC (Association Francaise de Genie Civil) (2013) "Ultra High Performance Fibre-Reinforced Concretes: Recommendations." Paris.

Amin, A., and Foster, S. J. (2016). "Shear strength of steel fibre reinforced concrete beams with stirrups." *Engineering Structures*, 111, 323-332.

Anderson, N. S., and Ramirez, J. A. (1989). "Detailing of stirrup reinforcement." *ACI Structural Journal*, 86(5), 507-515.

Bhal, N. S. (1968) "Uber den Einfluss der Balkenhöhe auf Schubtragfähigkeit von einfeldrigen Stahlbetonbalken mit und ohne Schubbewehrung." PhD thesis, University of Stuttgart.

Bresler, B. and Scordelis, A. C. (1963) "Shear strength of reinforced concrete beams." *ACI Journal Proceedings*, 60(1), 51-74.

Casanova, P., Rossi, P. and Schaller, I. (1997). "Can steel fibers replace transverse reinforcements in reinforced concrete beams?" *ACI Materials Journal*, 94(5), 341-354.

CEN (European Committee for Standardisation) (2004). “Eurocode 2: Design of concrete structures - Part 1-1: General rules and rules for building.” *EN 1992-1-1:2004*, Brussels,.

Chang, T. S. and Kesler, C. E. (1958) “Static and fatigue strength in shear of beams with tensile reinforcement.” *Journal of the American Concrete Institute,* 54(6), 1033-1057.

Chen, Y., Visintin, P., and Oehlers, D. J. (2015). “Concrete shear-friction material properties: Derivation from actively confined compression cylinder tests.” *Advances in Structural Engineering*, 18(8), 1173-1185.

Chana, P. S. (1981). “Some aspects of modelling the behaviour of reinforced concrete under shear loading.” *Tech. Rep. No. 543,* Cement and Concrete Association.

Choi, K. K., Hong-Gun, P., and Wight, J. K. (2007). “Shear strength of steel fiber-reinforced concrete beams without web reinforcement.” *ACI Structural Journal*, 104(1), 12.

Clark, A. P. (1951). “Diagonal tension in reinforced concrete beams.” ACI Journal Proceedings, 48(10), 145-156.

Collins, M. P. and Kuchma, D. (1999) “How safe are our Large, lightly reinforced concrete beams, slabs, and footings?” *ACI Structural Journal*, 96(4), 482-490.

Diaz de Cossio, R. and Seiss, C. P. (1960) “Behavior and strength in shear of beams and frames without web reinforcement.” *Journal of the American Concrete Institute*, 56(2), 695-736.

Diaz de Cossio R (1962). “Discussion to 326 report.” *ACI Journal Proceedings*, 59(11), 1323-1349.

Dönmez, A.A., Carloni, C., Cusatis, G., and Bažant, Z. P. (2020). “Size Effect on Shear Strength of Reinforced Concrete: Is CSCT or MCFT a Viable Alternative to Energy-Based Design Code?” *Journal of Engineering Mechanics*, 146(10), 04020110.

Elzanaty, A. H., Nilson, A. H., and Slate, F. O. (1986). “Shear capacity of reinforced concrete beams using high-strength concrete.” *ACI Journal Proceedings*, 83(2), 290-296.

fib (International Federation for Structural Concrete). (2013). “fib model code for concrete structures 2010.” Lausanne.

Frosch, R. J. (2000). “Behavior of large-scale reinforced concrete beams with minimum shear reinforcement.” *ACI Structural Journal*, 97(6), 814-820.

Harajli, M. H. (2009). “Bond stress–slip model for steel bars in unconfined or steel, FRC, or FRP confined concrete under cyclic loading.” *Journal of Structural Engineering*, 135(5), 509-518.

Kani, G. N. J. (1966) “Basic facts concerning shear failure.” *Journal of the American Concrete Institute*, 63(6), 675-692.

Kani, G. N. J. (1967) “How safe are our large reinforced concrete beams?” *Journal of the American Concrete Institute*, 64(3), 128-141.

Kim, W. and White, R. N. (1999) “Shear-critical cracking in slender reinforced concrete beams.” *ACI Structural Journal*, 96(5), 757-766.

Kotsovos, M. D. (1987) “Shear failure of reinforced-concrete beams.” *Engineering Structures*, 9(1), 32-38.

Krefeld, W. J. and Thurston, C. W. (1966) “Studies of the shear and diagonal tension strength of simply supported reinforced concrete beams.” *ACI Journal Proceedings*, 63(4), 451-476.

Kwak, Y. K., Eberhard, M. O., Kim, W. S., and Kim, J. (2002). “Shear strength of steel fiber-reinforced concrete beams without stirrups.” *ACI Structural Journal*, 99(4), 530-538.

Lantsoght, E. O. (2019). “Database of Shear Experiments on Steel Fiber Reinforced Concrete Beams without Stirrups.” *Materials*, 12(6), 917.

Lee, J.-Y., and Hwang, H.-B. (2010). “Maximum shear reinforcement of reinforced concrete beams.” *ACI Structural Journal*, 107(5), 580-588.

Lee, J.-Y., Choi, I.-J., and Kim, S.-W. (2011). “Shear behavior of reinforced concrete beams with high-strength stirrups.” *ACI Structural Journal*, 108(5), 620-629.

Lee, D.H., Han, S.J., Kim, K.S. and LaFave, J.M. (2016). “Shear capacity of steel fiber-reinforced concrete beams.” *Structural Concrete*, 18, 278-291.

Leonhardt, F. and Walther, R. (1962). “Schubversuche an einfeldrigen Stahlbetonbalken mit und ohne Schubbewehrung zur Ermittlung der Schubtragfähigkeit und der oberen Schubspannungsgrenze.” DAfStb.

Mathey, R. G. and Watstein, D. (1963) “Shear strength of beams without web reinforcement containing deformed bars of different yield strengths.” *Journal of the American Concrete Institute*, 60(2), 183-208.

Mattock, A. H. (1969). “Diagonal tension cracking in concrete beams with axial forces.” *Journal of the Structural Division*, 95(9), 1887–1900.

Mattock, A. H., and Wang, Z. (1984). “Shear strength of reinforced concrete members subject to high axial compressive stress.” *ACI Journal Proceedings*, 81(3), 287-298.

Melchers, R. E., and Beck, A. T. (2018). *Structural reliability analysis and prediction*. John Wiley & Sons.

Moody, K. G., Viest, I. M., Elstner, R. C. and Hognestad, E. (1954) “Shear strength of reinforced concrete beams part 1 -tests of simple beams.” *Journal of the American Concrete Institute*, 51(12), 317-332.

Morrow, J. and Viest I. M. (1957) “Shear strength of reinforced concrete frame members without web reinforcement.” *Journal of the American Concrete Institute*, 53(3), 833-869.

Mphonde, A. G. and Frantz, G. C. (1984) “Shear tests of high-strength and low-strength concrete beams without stirrups.” *Journal of the American Concrete Institute*, 81(4), 350-357.

Mphonde, A. G., and Frantz, G. C. (1985). “Shear tests of high- and low-strength concrete beams with stirrups.” *ACI Special Publication*, 87, 179-186.

Noghabai, K. (2000). “Beams of fibrous concrete in shear and bending: experiment and model.” *Journal of Structural Engineering*, 126(2), 243-251.

Olver, F. W., Lozier, D. W., Boisvert, R. F., and Clark, C.W. (2010) *NIST handbook of mathematical functions*. Cambridge University Press.

Papadakis, G. (1996) “Shear failure of reinforced concrete beams without stirrups.” PhD Thesis, Aristotle University of Thessaloniki.

Placas, A. and Regan, P. E. (1971) Shear failure of reinforced concrete beams. *ACI Journal Proceedings*, 68(10): 763-773.

Regan, P. E., and Yu, C. W. (1973). *Limit state design of structural concrete*. Chatto & Windus, London.

Sarsam, K. F., and Al-Musawi, J. M. S. (1992). “Shear design of high- and normal strength concrete beams with web reinforcement.” *ACI Structural Journal*, 89(6), 658-664.

Sozen, M. A., Zwoyer, E. M. and Siess, C. P. (1959) “Investigation of prestressed reinforced concrete for highway bridges. Part 1: strength in shear of beams without web reinforcement.” *Engineering Experimental Station Bulletin No. 452*, University of Illinois.

Standards Australia (2018). “Concrete Structures.” *AS3600:2018*. Sydney.

Sturm, A. B., Visintin, P., Oehlers, D. J. and Seracino, R. (2018) “Time dependent tension stiffening mechanics of fibre reinforced and ultra-high performance fibre reinforced concrete.” *Journal of Structural Engineering*, 144(8), 04018122.

Sturm, A. B. and Visintin, P. (2018) “Local bond slip behaviour of steel reinforcing bars embedded in UHPFRC.” *Structural Concrete*, 20(1), 108-122.

Sturm, A. B., Visintin, P., and Oehlers, D. J. (2019). “Rational design approach for the instantaneous and time-dependent serviceability deflections and crack widths of FRC and UHPFRC continuous and simply supported beams.” *Journal of Structural Engineering*, 145(11), 04019138.

Sturm, A. B., Visintin, P., and Oehlers, D. J. (2020) “Mechanics of shear failure in fibre reinforced concrete beams.” *Journal of Structural Engineering*, in press

Swamy, R. N., and Andriopoulos, A. D. (1974). “Contribution of aggregate interlock and dowel forces to the shear resistance of reinforced beams with web reinforcement.” *ACI Special Publication*, 42, 129-166.

Tang, C. W., Yen, T. and Chen, H. J. (2009) “Shear behavior of reinforced concrete beams made with sedimentary lightweight aggregate without shear reinforcement.” *Journal of Materials in Civil Engineering*, 21(12): 730-739.

Taylor, H. P. J. (1972) “Shear strength of large beams.” *Journal of the Structural Division,* 98(11), 2473–2490.

Tompos, E. J., and Frosch, R. J. (2002). “Influence of beam size, longitudinal reinforcement, and stirrup effectiveness on concrete shear strength.” *ACI Structural Journal*, 99(5), 559-567.

Visintin, P., Sturm, A. B., Mohamed Ali, M. S., and Oehlers, D. J. (2018). “Blending macro- and micro-fibres to enhance the serviceability behaviour of UHPFRC.” *Australian Journal of Civil Engineering*, 16(2), 106-121.

Völgyi, I., and Windisch, A. (2017). “Experimental investigation of the role of aggregate interlock in the shear resistance of reinforced concrete beams.” *Structural Concrete*, 18(5), 792-800.

Walraven, J. C. (1978) “The influence of depth on the shear strength of lightweight concrete beams without shear reinforcement.” *Rep. No. 5-78-4*, Delft University of Technology.

Watstein, D. and Mathey, R. C. (1958) “Strains in beams having diagonal crack.” *Journal of the American Concrete Institute*, 55(12), 717-728.

Wu, Y. F., and Hu, B. (2017). Shear strength components in reinforced concrete members. *Journal of Structural Engineering*, 143(9), 04017092.

Xie, Y., Ahmad, S. H., Yu, T., Hino, S., and Chung, W. (1994). “Shear ductility of reinforced concrete beams of normal and high-strength concrete.” *ACI Structural Journal*, 91(2), 140-149.

Yoon, Y.-S., Cook, W. D., and Mitchell, D. (1996). “Minimum shear reinforcement in normal, medium, and high-strength concrete beams.” *ACI Structural Journal*, 93(5), 576-584.

Yost, J. R., Gross, S. P. and Dinehart, D. W. (2001) “Shear strength of normal strength concrete beams reinforced with deformed GFRP bars.” *Journal of Composites for Construction*, 5(4), 268-275.

Zhang, J. P. (1997). “Diagonal cracking and shear strength of reinforced concrete beams.” *Magazine of Concrete Research*, 49(178), 55-65.

Zhang, T., Visintin, P., Oehlers, D. J., and Griffith, M. C. (2014a). “Presliding shear failure in prestressed RC beams. I: Partial-Interaction mechanism.” *Journal of Structural Engineering*, 140(10), 04014069.

Zhang, T., Oehlers, D. J., and Visintin, P. (2014b). “Shear strength of FRP RC beams and one-way slabs without stirrups.” *Journal of Composites for Construction*, 18(5), 04014007.

Zhang, T., Visintin, P., and Oehlers, D. J. (2016a). “Shear strength of RC beams without web reinforcement.” *Australian Journal of Structural Engineering*, 17(1), 87-96.

Zhang, T., Visintin, P., and Oehlers, D. J. (2016b). “Shear strength of RC beams with steel stirrups.” *Journal of Structural Engineering*, 142(2), 04015135.

Zhang, F., Ding, Y., Xu, J., Zhang, Y., Zhu, W., and Shi, Y. (2016c). “Shear strength prediction for steel fiber reinforced concrete beams without stirrups.” *Engineering Structures*, 127, 101-116.